Nitrogen GFIS-FIB secondary electron imaging: A first look

Marek E. Schmidt[1], Anto Yasaka[2,1], Masashi Akabori[1],Hiroshi Mizuta[1,3,4]

[1] School of Materials Science, Japan Advanced Institute of Science and Technology, Japan
[2] Hitachi High-Tech Science Corp., Japan
[3] Nanoelectronics and Nanotechnologies Research Group, Electronics and Computer Science, Faculty of Physical Sciences and Engineering, University of Southampton, UK
[4] Institute of Microengineering and Nanoelectronics, Universiti Kebangsaan Malaysia, Malaysia

Supplementary Information

1. Device fabrication

Five of the six samples used in this work (C2-C6) were fabricated using different processes as illustrated in Figure S1. In this section, details about the individual process steps are provided. All lithographic steps were done by direct e-beam lithography.

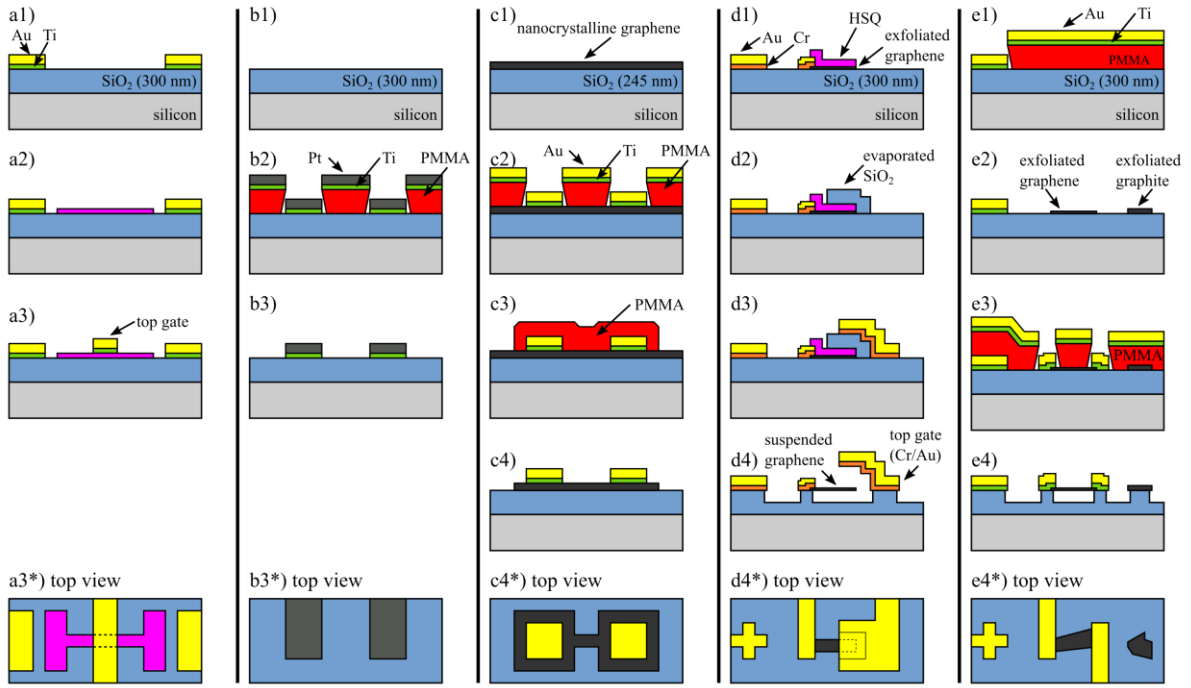

Figure S1: Schematic fabrication process charts for samples used in this work. (a) C2: Fabrication of buried graphene with top gate. A suspended top-gate is fabricated above parts of the graphene cantilever. (b) C3: Ti/Pt structures are deposited on SiO_2 by the lift-off technique. (c) C4: Fabrication of nanocrystalline graphene (NCG) sample. (d) C5: Fabrication of exfoliated graphite/graphene device with suspending and top gate. (e) C6: Fabrication of suspended graphite/graphene device.

1.1.Sample C2: HSQ on SiO_2 with top gates

Alignment structures are patterned by lithography (MMA/PMMA bi-layer resist) and Ti/Au lift-off in N-Methyl-pyrrolidone (NMP) on a SiO_2 substrate as shown in Figure S1a1. Next, a hydrogen silsesquioxane (HSQ) hard mask is patterned (Figure S1b2). Another Ti/Au lift-off process is used to define top gates (Figure S1a3).The top view in Figure S1a3* shows a characteristic HSQ structure with the top gate.

1.2.Sample C3: Ti/Pt structures

The fabrication process of the sample with thin Ti/Pt structures on 300 nm SiO_2 substrate is illustrated in Figure S1b. PMMA-based lithography is used to define several structures with sizes from few micrometers to few hundreds of micrometers. After electron-beam evaporation of 3/12 nm of Ti/Pt, lift-off in NMP is performed (Figure S1b2+3). Afterwards, the sample was cleaned in an oxygen plasma asher (200 Watt) to remove resist residues.

1.3.Sample C3: Nanocrystalline graphene

Large-area nanocrystalline graphene with a thickness of ~50 nm was deposited by metal-free plasma-enhanced chemical vapor deposition (PECVD) directly onto SiO_2 [3], and consecutively thinned to ~5 nm by oxygen inductively coupled plasma reactive ion etching (ICP-RIE, Ar gas flow: 40 sccm, oxygen gas flow: 5 sccm, pressure: 4 Pa, RF power: 30 W, Bias

power: 10 W, etch duration: 170 sec) as shown in Figure S1c1. MMA/PMMA-based lithography and lift-off in NMP was used to deposit Ti/Au contact pads and alignment structures directly onto the NCG film (Figure S1c2), followed by patterning of a PMMA etching mask and NCG channel formation using O_2 ICP-RIE. Finally, the remaining etching mask was removed by acetone and the sample was annealed in H_2/Ar atmosphere at 300°C for 2 hours to improve electrical contacts between NCG and contact pads, as well as removing organic surface contaminants.

1.4. Sample C5: Suspended exfoliated graphene with top gate

After patterning alignment structures by lithography (MMA/PMMA bi-layer resist) and Cr/Au lift-off in N-Methyl-pyrrolidone (NMP), graphene was exfoliated from Kish graphite onto the 300 nm thermally oxidized silicon samples. The technique of mechanical exfoliation from graphite is well-established [1], and yields an abundant number of random flakes with varying thickness (the number of graphene layers can vary even in one flake), size and shape (flakes can comprise folds). Next, selected flakes (mainly mono- and bi-layer graphene) are electrically contacted by PMMA lithography and consecutive Ti/Au lift-off in NMP. Other flakes are left electrically isolated. Next, a hydrogen silsesquioxane (HSQ) etch mask is patterned on the contacted graphene to define the shape of the final device, and reactive ion etching (oxygen flow rate: 10 sccm, pressure: 26.5 Pa, power: 75 Watt, duration: 30 seconds) is used to etch away the unprotected graphene (compare Figure S1d1). Next, 75 nm of SiO_2 (electron-beam evaporation) are patterned by PMMA-based lift-off to form a sacrificial layer (Figure S1d2) and the top gate (Cr/Au) is patterned by another PMMA-based lift-off step as shown in Figure S1d3. Finally, the structure is released by buffered HF etching (90 seconds) and consecutive drying in a critical point drier. The etch rate of thermally grown SiO_2 in BHF solution is around 100 nm/min, meaning that SiO_2 remains on the sample as depicted in Figure S1d4 and Figure S1d4*, respectively.

1.5.Sample C6: Suspended exfoliated graphene

After preparing a sample the same way as for sample C5 (Figure S1e1-e3), a PMMA etch mask is patterned that only reveals selected areas that help to shape previously selected mono- and bi-layer graphene flakes into defined widths. Finally, the structure is released by buffered HF etching (90 seconds) and consecutive drying in a critical point drier. This step iss depicted in Figure S1e4 and Figure S1e4*, respectively.

2. Imaging conditions

Below is a detailed list of the imaging condition used during acquisition of the GFIS-FIB SE images in this work.

Image	Gas species	Current [pA]	Pixel spacing [nm]	Pixel dwell time [µs]
2a	N2	0.28	3.75	300
2b	He	1.4	3.75	100
2c	N2	0.218	1.25	50
2d	He	0.245	1.25	50
2e	N2	1.25	200	10
2f	He	1.7	200	50
2g	N2	1.16	3.75	10
2h	He	1.7	3.75	50
3a	N2	0.08	400	50
3b	He	0.18	800	100
5a	N2	0.03	12.5	80
6a	N2	1.14	12.5	5
6b	He	0.066	12.5	100
6c	N2	1.14	12.5	200
6g	N2	1.14	50	20
8a	N2	0.192	200	20
8b	N2	0.192	12.5	5
8c	N2	0.192	12.5	20
8d	N2	0.192	12.5	100
8e	N2	0.192	12.5	500
8f	N2	0.192	3.75	100

3. Histograms of SE images from Figure 6

The Normalized SiO2/graphite contrast values shown in Figure S2f of the main text. As some of the SE intensity profiles are of low SNR, we evaluate additionally the distribution of pixel intensities (grey values) based on statistic evaluation. For this purpose, several areas were defined in ImageJ that exclude defective and edge areas of the four materials found in the images, namely Au, SiO_2, graphite and graphene, respectively. The Location and shape of these areas is shown in Figure S2d. The histograms in these areas was extracted using ImageJ from the original, unmodified SE images and are shown in Figure S2a-c. Note that black pixels are attributed an intensity of 1. The distributions for Au and SiO_2 follows a normal distribution in the high dose nitrogen and helium image. In the low dose nitrogen image we do not observe this, meaning that the intensity of many pixels was too low to exceed

the required detection threshold of the SE detector. Please refer to the discussion of the effective dose in the main text that explains the reason for this observation although the dose of the helium and nitrogen image are very similar. For graphite and graphene we observe normal distribution only in the helium image, while the two nitrogen images show a dominant number of pixels with lowest intensity. For the low nitrogen dose histograms no fitting was done, but the man intensities for high dose nitrogen and helium image are tabulated as inset of the histogram figures. The normal distribution curves are shown as well. Using these values, we calculate normalized SiO_2/graphite contrast of 1.24 and 0.45 for the high dose nitrogen and helium histogram, respectively. This is a ~200% improved value for nitrogen, which is lower than the ~370% obtained from averaging. This is mainly due to the inaccurate fitting of the graphite histogram, and supports the discussion made in the main text.

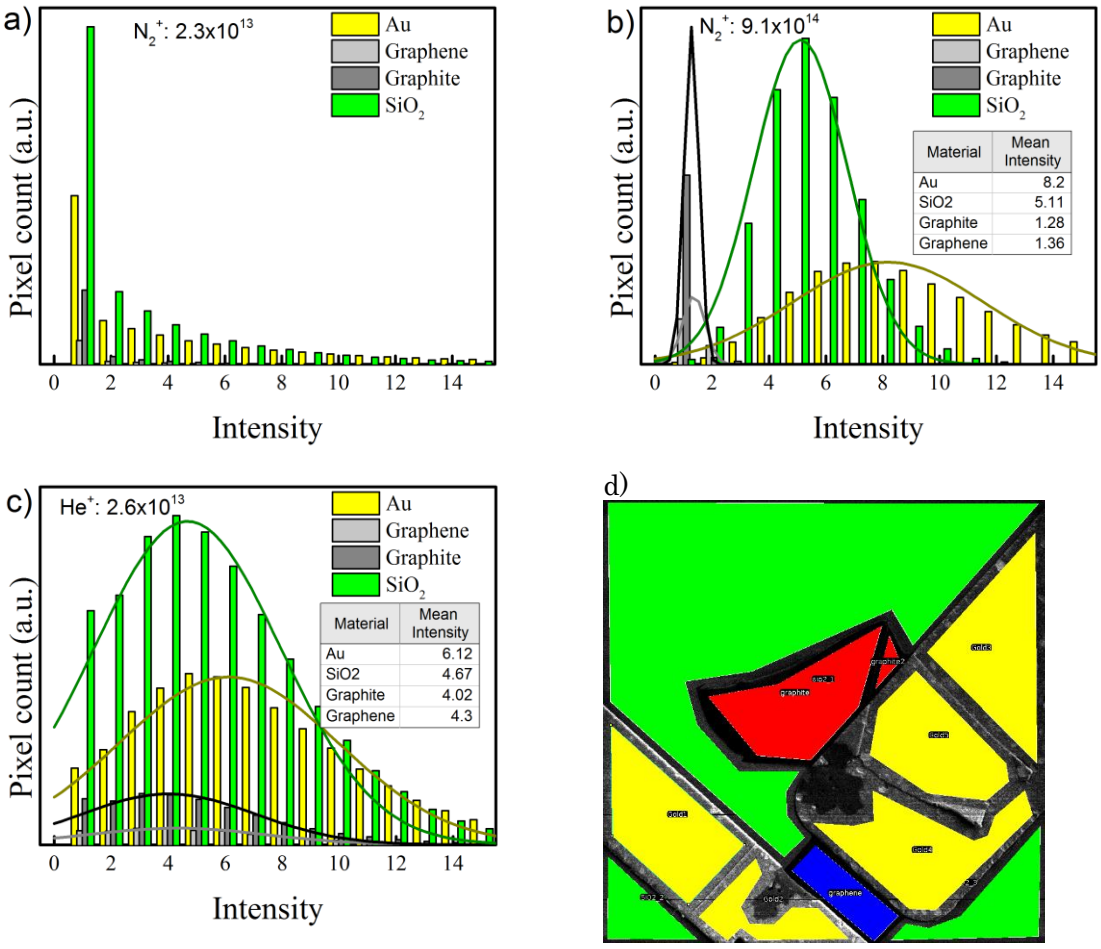

Figure S2: Histograms extracted from original, unmodified versions of SE images reported in Figure 1. (a) Low nitrogen dose histogram does not show normal distribution of intensities. (b) High nitrogen dose with normal distribution for gold and SiO_2. A normalized SiO_2/graphite contrast of 1.24 is calculated from the mean intensity values. (c) Helium GFIS-FIB image showing normal distributed intensities for all four materials. A normalized SiO_2/graphite contrast of 0.45 is calculated. (d) Illustration of the individual areas used for histogram extraction. Defect and edge areas are excluded. Yellow: Au, green: SiO_2, red: graphite, blue: graphene.

4. Sample topography

Atomic force microscopy (SII SPA400, dynamic mode) was used on samples C1 and C4 to extract the surface topography.

4.1. Sample C1

The film thickness and step heights on sample C1 were extracted using Gwyddion[4] from the AFM image shown in Figure S3a. The relevant step height profiles are shown in Figure S3b. The height of the suspended air gap (~90 nm) is extracted from the step height of Profile 1 (~194 nm) and the process parameters used during fabrication (100 nm Au + 5 nm Cr). The

gap is smaller (50 nm) at the location of Profile 2, which is due to bending down of the gold. This gap is also observed for Profile 4. The thickness of the graphite is 40-45 nm, which is extracted from the kink location of Profile 4, and Profile 5 (graphite step below the Au layer).

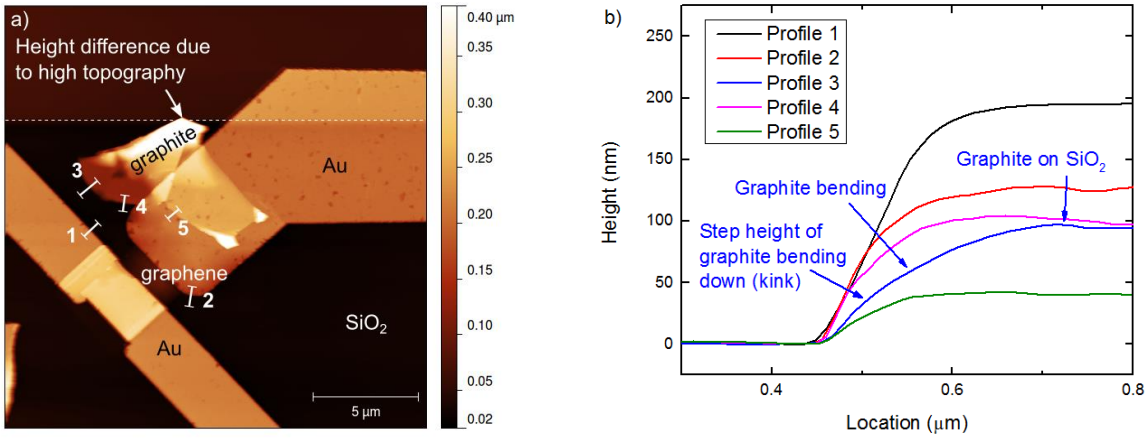

Figure S3: Sample C1 (a) AFM image and (n) height profiles along the lines indicated in (a).

We furthermore extracted root mean square (RMS) roughness values for the graphite, graphene, SiO_2 (exposed and unexposed), as well as Au (exposed and unexposed), were obtained by Gwyddion from 500x500 nm^2 scans in random locations. The values are summarized in

Table S1, and some selected AFM images are shown in Figure S4. For the graphene and graphite, no unexposed data exists. For SiO_2 and Au we observe a moderate roughness increase of 52% and 21%, respectively.

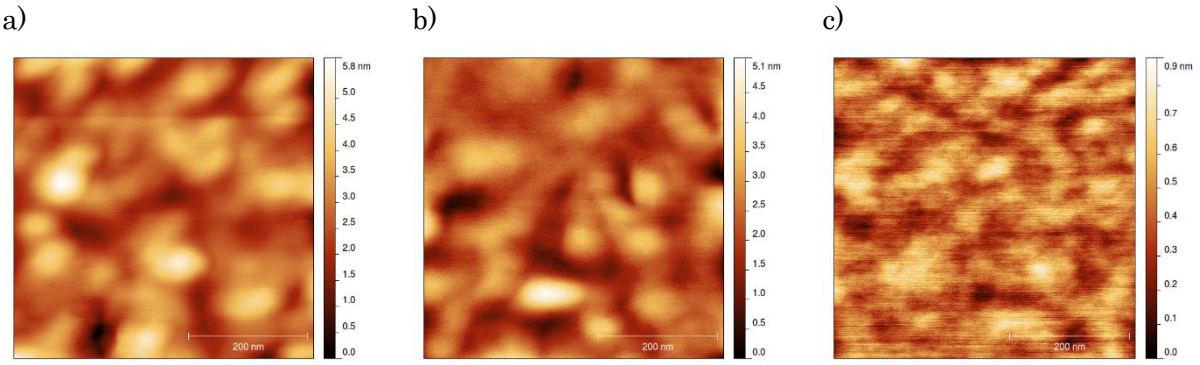

Figure S4: Sample C1. Representative 500x500 nm^2 AFM scans of (a) Au inside the imaged area (RMS 0.766 nm), (b) Au far away from the imaged area (RMS 0.629 nm) and (c) SiO_2 far away from the imaged area (RMS 0.118 nm).

Table S1: Root mean square roughness values extracted from AFM measurements on sample C1.

Material	RMS (unexposed)	RMS (exposed)	Change
Graphene	-	0.373 nm	-
Graphite	-	0.545 nm	-
SiO_2	0.118 nm	0.180 nm	+ 52%
Au	0.629 nm	0.766 nm	+ 21%

4.1.Sample C3 (NCG)

The AFM topography image of sample C4 (channel region) is shown in Figure S5. The roughness values are summarized in Table S2.

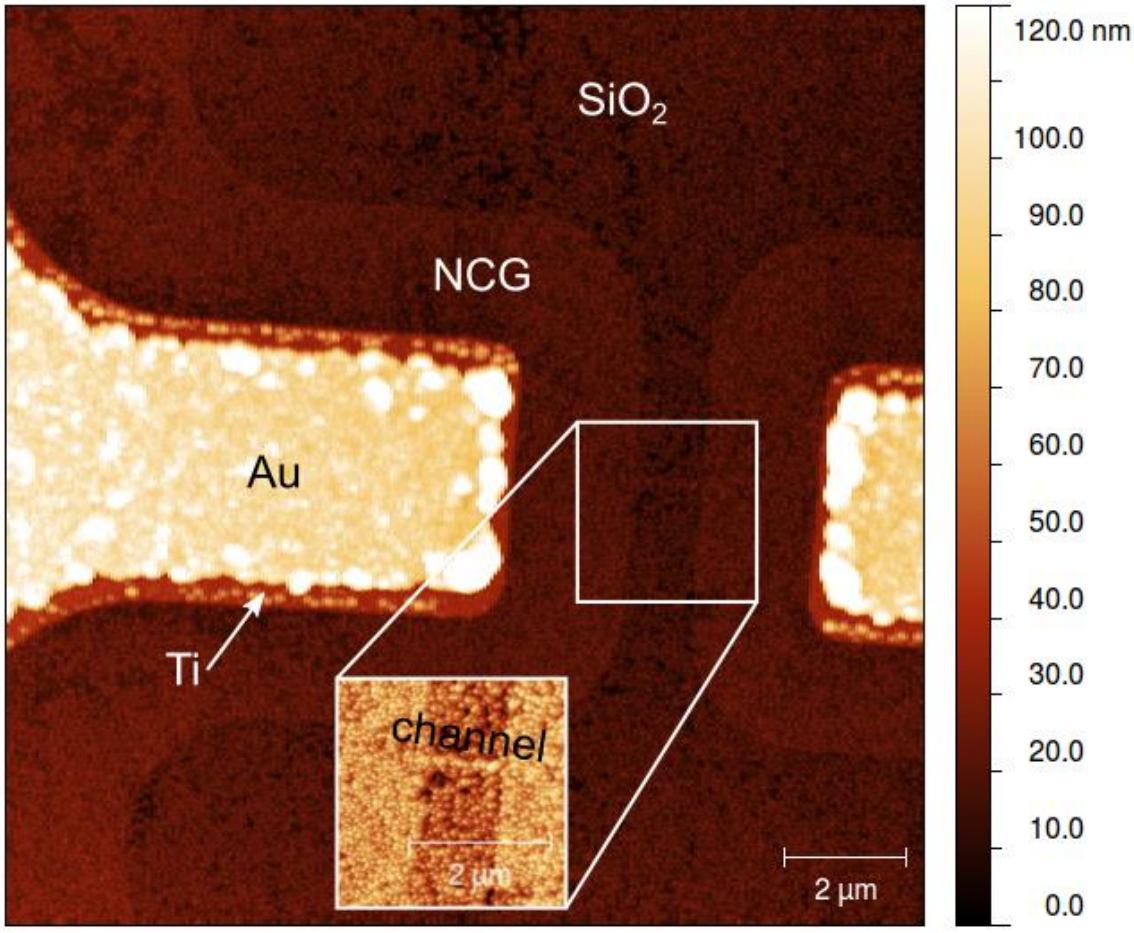

Figure S5: Sample C4. AFM image of the imaged area with NCG, Ti and Au. The rough edges and surface defects of the Au are caused during the infrared furnace annealing.

Table S2: Root mean square roughness values extracted from AFM measurements on sample C4.

Material	RMS
NCG	3.4 nm
SiO_2	4.3 nm
Au	6.6 nm
Ti	2.4 nm

4.2.Sample C4 (Exfoliated graphite)

The AFM topography image of sample C4 (compare Figure 4a-c of the manuscript) is shown in Figure S6. The thickness t = 25 nm of the graphite is extracted from Profile 1. Profile 2 is taken across the top part of the graphite flake, with a thickness of 6-8 nm.

a) b)

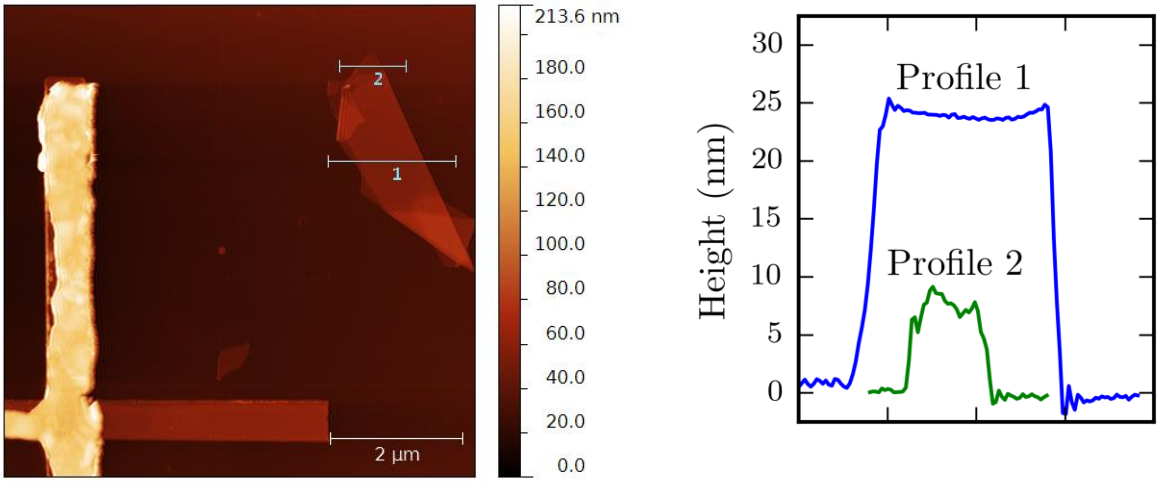

Figure S6: Sample C2. (a) 7x7 µm² AFM scan of the imaged area of sample C2 shown in Figures 4a-c. (b) Height profiles shown in (a).

5. References

[1] A. K. Geim and K. S. Novoselov, "The rise of graphene," *Nat Mater*, vol. 6, no. 3, pp. 183–191, Mar. 2007.

[2] "Graphene Platform Corp. Website," *GRAPHENE PLATFORM*. [Online]. Available: http://grapheneplatform.com. [Accessed: 08-Dec-2014].

[3] M. E. Schmidt, C. Xu, M. Cooke, H. Mizuta, and H. M. H. Chong, "Metal-free plasma-enhanced chemical vapor deposition of large area nanocrystalline graphene,"

Mater. Res. Express, vol. 1, no. 2, p. 025031, Apr. 2014.

[4] D. Nečas and P. Klapetek, "Gwyddion: an open-source software for SPM data analysis," *Cent. Eur. J. Phys.*, vol. 10, no. 1, pp. 181–188, Nov. 2011.